

PACS numbers: 42.65.Ky; 42.55.Rz; 52.50.Jm; 79.20.Eb
DOI: 10.1070/QE2012v042n10ABEH014931

High-order harmonic generation of picosecond radiation of moderate intensity in laser plasma

G.S. Boltaev, R.A. Ganeev, I.A. Kulagin, N.Kh. Satlikov, T. Usmanov

Abstract. **The results of investigations into the generation of high-order harmonics (up to the 21st order) of picosecond (τ = 38 ps) Nd:YAG laser radiation in the plasma produced by laser ablation of metal and carbon-containing material surfaces are presented. We demonstrate the feasibility of generating high-order harmonics in the vacuum ultraviolet spectral range (with radiation wavelengths shorter than 120 nm) in plasmas with an efficiency of $\sim 0.7 \times 10^{-4}$. In carbon-containing plasma, the 7th harmonic intensity exceeded that of the 5th one by a factor of seven.**

Keywords: *high-order harmonic generation, picosecond radiation, laser plasma, metals, carbon-containing materials.*

1. Introduction

The last two decades have seen intensive research in the area of high-order harmonic generation (HOHG) of laser radiation. The technical impetus to the pursuance of these investigations was lent by the development and fabrication of high-power radiation sources of femtosecond duration [1, 2]. The high radiation intensity achieved for relatively small dimensions and simplicity of such laser sources has made it possible to radically increase the maximum harmonic order and discuss practical applications of coherent short-wavelength radiation to plasma diagnostics, biology, microscopy, photolithography, etc. The increase in generated harmonic order provides a promising technique for producing soft X-ray radiation [3, 4], which furnishes an alternative to X-ray lasers and free-electron lasers [5, 6]. At present there exist two main methods of HOHG: in gaseous media and from the surface of a solid target. The former method, unlike the latter one, does not require ultrahigh light field intensities, and the intensity of laser radiation usually involved in this case does not exceed 10^{15} W cm^{-2}. HOHG in rare gases significantly broadened the spectral range of obtainable coherent radiation, which now extends to the water transparency window (2.3–4.6 nm and below) required in biological research, and provided the basis for producing attosecond pulses [7].

However, despite the diversity of duration and intensity ranges of the laser radiation involved [8, 9], the energy efficiency of conversion to harmonic radiation remains low (10^{-5}–10^{-7}). In the framework of the three-stage model, according to the well-known law for the limiting generated photon energy [10] $\hbar\omega_b \approx I + 3U_p$ (here, I is the ionisation potential, U_p is the ponderomotive electron energy in the laser field), for the same laser radiation intensity the short-wavelength bound may be made shorter by using media with a higher ionisation potential. For this purpose, attempts were made to use particles with a high ionisation potential, plasma ions in particular [11–13]. Using plasmas opens far broader possibilities for varying the parameters of a nonlinear medium, because plasma media are more numerous than the gaseous ones. In the initial experiments, however, attempts to raise the limiting harmonic photon energy and improve the HOHG efficiency did not meet with success. More recent investigations showed that it is expedient to employ low-temperature and weakly excited plasmas as the nonlinear media for HOHG in the vacuum ultraviolet and soft X-ray ranges [14, 15]. Using plasmas for realising the optimal conditions enabled increasing the highest generated harmonic order (up to the 101st harmonic) as well as the HOHG efficiency under close-to-resonance conditions (up to $\sim 10^{-4}$ in some spectral ranges) [16, 17]. Despite certain successes in HOHG, the energy efficiency of conversion to high-order harmonics nevertheless remains at a level suitable only for diagnostic purposes. In this connection, attempts persist to develop new techniques and find new media for raising the efficiency and energy of high-order harmonic radiation [18–20].

For the same HOHG efficiency, the harmonic energy density with the use of picosecond pulses is evidently higher than that with femtosecond laser radiation due to a higher energy of pulses in the former case. Furthermore, the relatively low cost of picosecond facilities is conductive to the practical application of these vacuum UV and soft X-ray sources.

In the present work we investigated the efficiency of high-order harmonic generation for picosecond Nd:YAG laser radiation in plasmas produced by laser ablation of the surfaces of some metals and carbon-containing materials. The parameters of the medium and laser radiation were optimised in order to maximise the energy density of harmonic radiation in the 50–220-nm wavelength range. We also analysed the possibilities and mechanisms for improving the HOHG efficiency in these media.

2. Experimental facility

For a radiation source use was made of a passively mode-locked Nd:YAG laser (λ = 1064 nm) which generated a train of 38-ps long pulses with a pulse repetition rate of 1.5 Hz (Fig. 1). Upon extraction of a single pulse and its amplification in two amplifiers, the radiation was split into two parts. The first part of the radiation (with a pulse energy of $\sim$5 mJ) was used

G.S. Boltaev, R.A. Ganeev, I.A. Kulagin, N.Kh. Satlikov, T. Usmanov Institute of Ion-Plasma and Laser Technologies, Uzbekistan Academy of Sciences, Akademgorodok, 100125 Tashkent, Uzbekistan; e-mail: ilya_kulagin@list.ru, rashid_ganeev@mail.ru, timurbek_usmanov@mail.ru

Received 25 May 2012; revision received 16 July 2012
Kvantovaya Elektronika **42** (10) 899–906 (2012)
Translated by E.N. Ragozin

as a heating pulse and was directed via a focusing lens to the surface of a target located in a vacuum chamber. The highest intensity of the heating pulse in use was equal to $\sim 10^{11}$ W cm^{-2}. After a certain time delay, the second part of the laser pulse (the probe pulse with an energy of 28 mJ) was focused, parallel to the target surface, into the plasma plume. The peak intensity of the probe pulse was equal to 4×10^{13} W cm^{-2}. To determine the optimal time delay between the pulses, we investigated the efficiency of HOHG for different delays in the 5–150-ns range. The radiation of the probe pulse and high-order harmonics were separated in a VMR-2 vacuum monochromator. The harmonic radiation in the 50–300-nm range was recorded with a scintillator (sodium salicylate, SS) and a photomultiplier (PM).

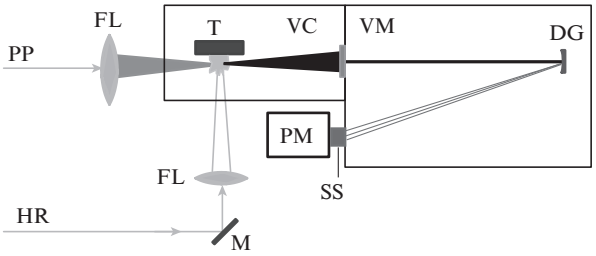

Figure 1. Schematic of the experimental facility: (PP) picosecond probe radiation; (HR) picosecond heating radiation; (M) mirror; (FL) focusing lenses; (VC) vacuum chamber; (T) target; (VM) vacuum monochromator; (DG) diffraction grating; (SS) sodium salicylate; and (PM) photomultiplier.

The targets were plates of size $5 \times 5 \times 2$ mm. For a target material, use was made of different metals (copper, chromium, zinc, molybdenum, titanium, tin, lead, tantalum, manganese, gold, silver, boron, and aluminium) as well as of carbon-containing materials (graphite, vitreous carbon, pyrolitic graphite, boron carbide, silicon carbide, and a pencil core). To change the target position and accordingly the probing radiation–plasma interaction region relative to the target plane, use was made of a three-dimensional manipulator.

3. Plasma emission spectra

Important information about plasma parameters can be gained by analysing its emission spectra. Below we analyse the time-averaged plasma emission spectra of different metals and carbon-containing materials employed for HOHG in the propagation of the picosecond probe radiation through the plasma plume. These investigations were aimed at determining the optimal conditions for the production of plasma objects in order to maximise the HOHG efficiency. The atomic and ionic emission spectra of the laser plasmas were analysed in the visible and UV ranges (300–700 nm). An HR4000 fibre spectrometer was employed to record the plasma emission spectra.

Figure 2a shows the emission spectrum of the plasma produced on the surface of a zinc plate, which corresponds to the 'optimal plasma' production conditions (from the standpoint of maximising the efficiency of HOHG). To this end, we maximised the harmonic efficiencies in the 80–200-nm range and then determined the spectral characteristics of the laser plasma produced under these conditions. One can see from

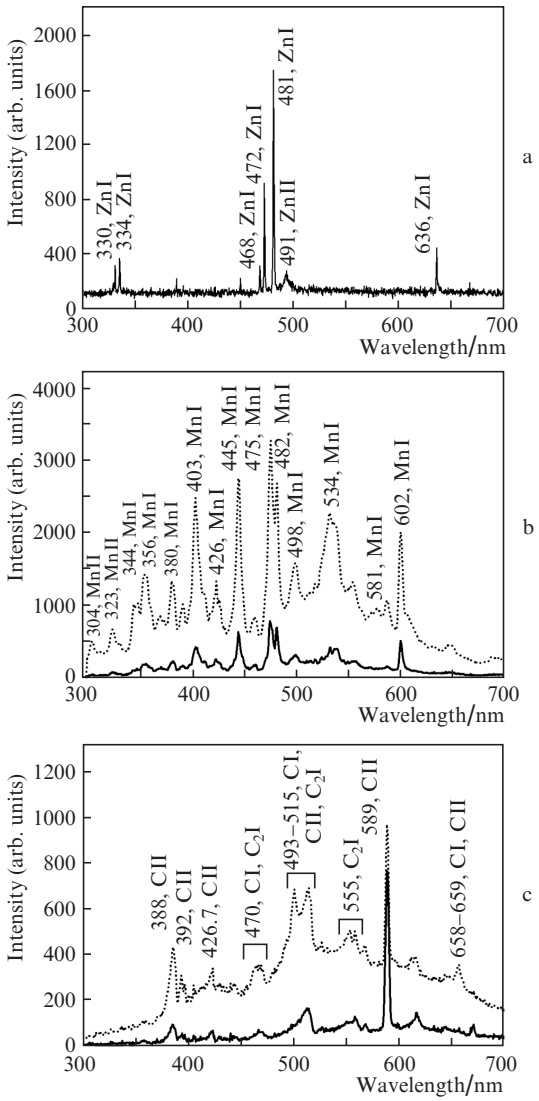

Figure 2. Emission spectra of zinc (a), manganese (b), and graphite (c) plasmas.

the figure that the recorded spectral lines arise primarily from transitions between the states of neutral atoms and singly charged ions.

In the irradiation of the metals, increasing the intensity of the heating pulse above 10^{11} W cm^{-2} resulted in an increase of the emission intensity of neutral atoms and singly charged ions and in spectra broadening as well as in the emergence of new spectral lines inherent in higher-multiplicity ions. As a result of the changes in the plasma composition, the HOHG efficiency significantly lowered in practically all plasma objects under study. The spectra of plasma emission at a high intensity of the heating pulse are shown in Figs 2b and 2c. The solid and dotted lines correspond to the weak and strong target excitations. Also evident are structural changes in the spectra and changes in the radiation intensity of the plasma produced on the surface of manganese and graphite targets.

The ionisation potentials of the atoms and singly charged ions of carbon are higher than the ionisation potentials of the metals and are equal to 11.25 and 24.38 eV, respectively. In the case of optimal graphite ablation, the carbon plasma consists almost completely of neutral atoms and singly charged ions, which is borne out by our measurements of the emission

spectra in the visible and UV ranges (Fig. 2c). This figure shows the spectral lines typical for the majority of carbon-containing materials used in our study, which arise from transitions between the states of C I and C II. Also observed in the spectra were the excited states of C_2.

Our subsequent investigations showed that the excessive plasma excitation in the course of laser ablation is responsible for a drastic lowering of HOHG efficiency for the majority of plasma objects; however, in individual cases this can result in an increase in the highest harmonic order.

4. Optimisation of HOHG in plasma

In the first series of experiments we analysed the effect of probe radiation polarisation on the efficiency of HOHG. Figure 3 shows the intensities of the 5th and 7th harmonics as functions of the rotation angle of a quarter-wave plate, which changed the polarisation of the probe radiation from a linear polarisation (for 0°) to a circular one (for 45°). A small deviation from the linear polarisation resulted in a significant lowering in the intensity of harmonic radiation. In the case of circularly polarised radiation, the harmonic radiation vanished, which corresponds to the theory of harmonic generation in isotropic media [21].

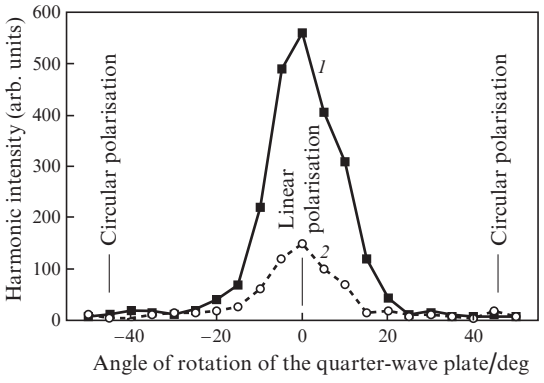

Figure 3. Dependences of the 5th (*1*) and 7th (*2*) harmonic intensities from the pyrolitic graphite plasma on the angle of rotation of the quarter-wave plate.

To optimise the HOHG, we analysed several harmonic properties in the plasma produced by laser ablation. An important parameter of HOHG optimisation is the time delay between the heating pulse and the probing one. Figure 4 displays the typical dependences of the intensity of a harmonic on the time delay between these pulses for carbon, manganese, and lead plasmas. Early in the plasma formation and expansion from the target surface, the particle density (the density of neutral atoms and singly charged ions) in the zone of interaction with the probing radiation was not high enough, because the plasma particles did not manage to reach the axis of probing radiation propagation, which was spaced at ~100 μm from the target surface. When the time delay was made equal to the time taken for the plasma particles to reach the interaction zone, the HOHG efficiency became higher. The subsequent lengthening of the time delay resulted in the saturation of HOHG and eventually in a lowering of the efficiency for long time delays.

An analysis of Fig. 4 suggests that the optimal time delays are different for different plasmas: for the C, Mn, and Pb

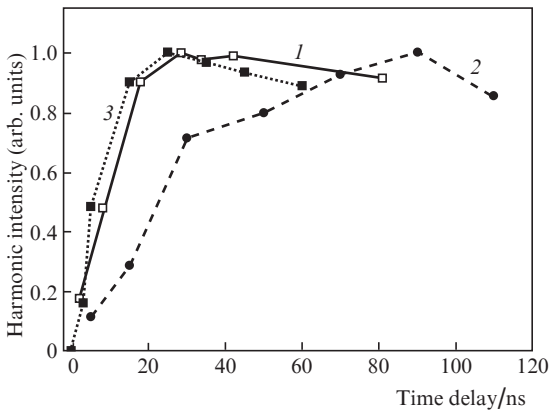

Figure 4. Harmonic intensities as functions of the time delay between the heating and probe pulses in manganese (*1*), lead (*2*), and graphite (*3*) plasmas.

plasmas they were equal to 25, 30, and 90 ns, respectively. The difference in time delay arises from the difference in the initial velocity of the particles of different elements. According to the hydrodynamic plasma evaporation model with gas-dynamic boundary condition [22], the initial velocity of the particles is defined by their mass, their binding energy in a solid, the Debye frequency, and the absorbed intensity of laser radiation. In the framework of this model, the initial velocity of atomic lead particles is lowest among the investigated materials for the same absorbed intensity of laser radiation. Therefore, efficient HOHG in lead will be observed for a longer time delay between the heating and probe pulses in comparison with targets made of materials with a lower atomic number. The highest initial velocity and accordingly the shortest time delay must take place in aluminium plasmas. Therefore, the optimal time delay may shorten with increase in the intensity of the heating pulse. However, the degree of plasma excitation increases in this case. Under the conditions of strong excitation, in the majority of plasmas investigated in our work we observed only a limited number of harmonics with lower conversion efficiencies.

We measured the dependence of HOHG efficiency on the energy of the heating pulse for the same dimensions of the beam waist at the target surface (~500 μm) (Fig. 5). In particular, the 5th harmonic signal generated in the Mn plasma was observed to decrease when the energy of heating pulses exceeded 1.5 mJ (Fig. 5a). In the lead plasma, we observed a lowering of 11th harmonic signal when the energy exceeded 3 mJ, which corresponds to an intensity of 10^{11} W cm^{-2} (Fig. 5b). In the plasma generated at the surface of pyrolitic graphite, the 7th harmonic signal lowered when the energy of heating pulses exceeded 6.5 mJ (Fig. 5c). A common feature of these dependences is a sharp lowering of harmonic intensity when the surface is irradiated by a heating pulse with an energy exceeding a certain level. The reason lies with excessive plasma excitation, which is responsible for the emergence of free electrons and multiply charged ions and to the corresponding phase mismatch between the probing radiation and harmonic waves. This effect is more significant for the generation of low-order harmonics. It is noteworthy that a lowering of the efficiency of laser frequency conversion in a highly excited plasma was earlier observed for harmonics of far higher orders [23], although the efficiency lowering was smaller than in the present investigation.

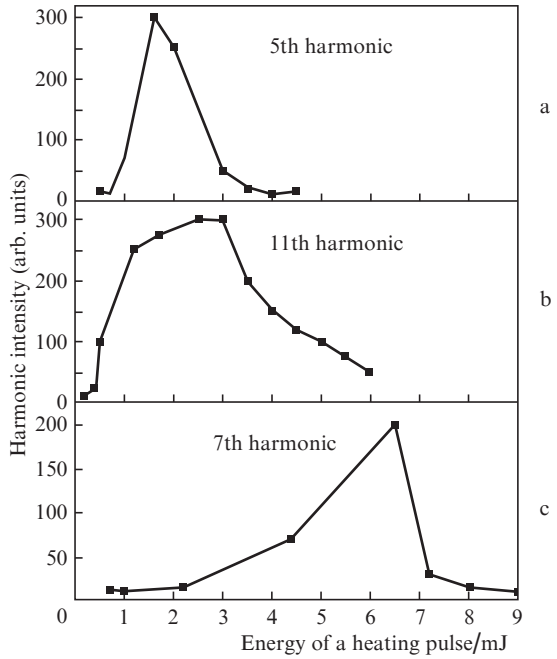

Figure 5. Optimal energy of the heating pulse in manganese (a), lead (b), and graphite (c) plasmas.

5. High-order harmonic distribution

A common feature of practically all spectral dependences of the harmonics generated in excessively excited metal plasmas was a characteristic lowering of the conversion efficiency – a sharp lowering for low-order harmonics and a gradual one for higher-order (above the 9th) harmonics, up to the short-wavelength bound (~50 nm, the 21st harmonic) of the monochromator operating range. Figure 6 shows typical HOHG spectra recorded from Sn, Cr, Al, and C plasmas. The efficiency of HOHG in Sn and Cr plasmas was respectively highest and lowest throughout the spectral harmonic distribution range (Figs 6a and 6b) in comparison with other materials. We emphasise that, despite significant dissimilarity of materials, the majority of investigated plasmas exhibited comparable efficiency values.

Although the majority of plasma did exhibit similar properties in the course of HOHG, in some materials we observed nontrivial spectral harmonic distributions. In particular, in some instances no harmonics above the 9th one were generated within the detection range. For instance, this behaviour was exhibited by the plasma produced on the surface of aluminium (Fig. 6c).

The absolute conversion efficiency was measured by the following technique. At the first stage, a recording system 'monochromator + sodium salicylate + PM' was used to measure the signal of the 4th harmonic (with a wavelength of 266 nm) with a known energy, which was generated in nonlinear crystals. This enabled calibrating the recording system for harmonics in this spectral region. Since the luminescence quantum efficiency of sodium salicylate is constant over a broad spectral range (30–350 nm), calibrating the recording system in the 266-nm region permitted us to calculate the absolute conversion efficiencies for higher-order harmonics. The conversion efficiencies for plasmas generated on the metal surfaces are collected in Table 1.

Figure 6d shows the harmonic distribution for the plasma generated on the surface of graphite, which is typical for the carbon-containing materials under study. An interesting feature of the observations is the relatively high generation efficiency of the 7th harmonic, which prevails over the remaining ones. This efficiency is significantly (four–eight times) higher than the generation efficiency of the lower, 5th, harmonic,

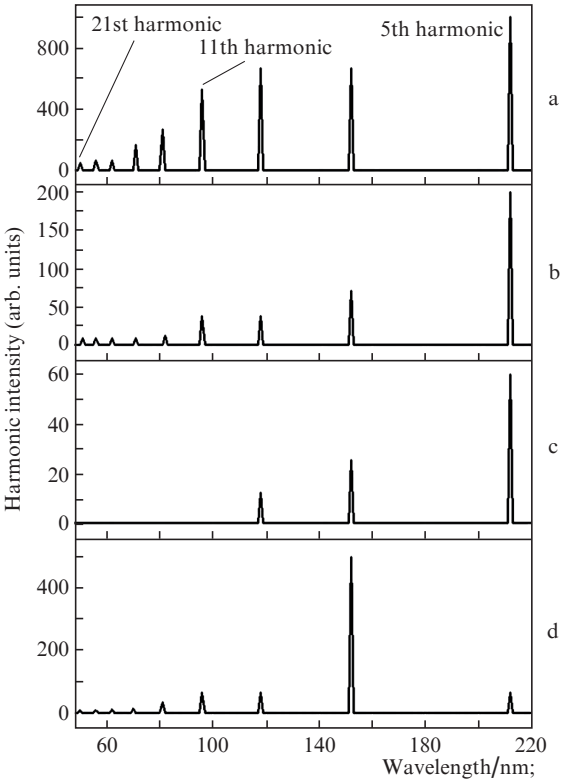

Figure 6. Spectral high-order harmonic distribution in tin (a), chromium (b), aluminium (c), and graphite (d) plasmas.

Table 1. Conversion efficiencies in metal plasmas ($\times 10^{-6}$).

Harmonic number	Wavelength/ nm	Sn	Zn	Mn	Ti	Cu	W	Au	B	Ta	Ag	Cr	Mo	Si	Al
5	213	100	80	80	70	46	46	40	40	26	20	20	4.2	3.83	6
7	152	66	66	20	20	33	40	33	13	10	16	7.1	3.8	1.75	2.59
9	118	66	53	10	12	15	38	26	3	3	10	3.8	2.5	1.75	1.33
11	97	53	40	6.6	6.6	13	33	20	1.3	1.8	6.6	3.8	2.1	0.91	
13	82	26	4	2.1	4.6	2.5	7	1.8	1	0.9	2.6	1.3	0.9	0.91	
15	71	16	4	1.75	3.3	0.9	5	1.3		0.9	1.3	0.9			
17	63	6	1.7	1.3	2.1	0.9		1.3		0.9	1	0.9			
19	56	6	1.7	1.3	2.1	0.83		0.9		0.75	1	0.9			
21	51	4	1	1.3	2.1	0.75		0.9		0.75	1	0.9			

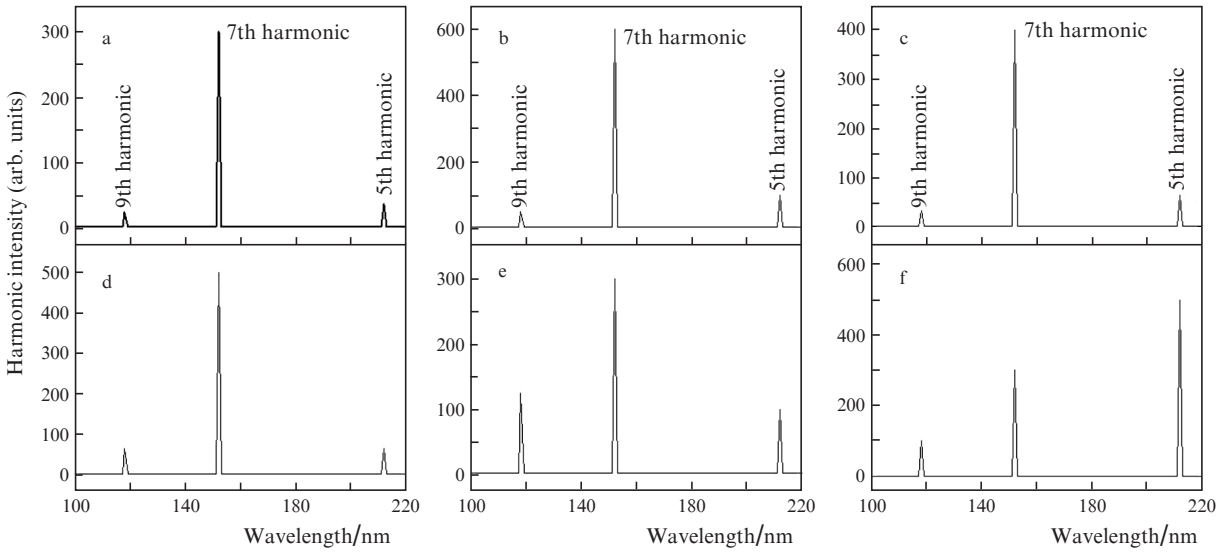

Figure 7. 5th, 7th, and 9th harmonic intensity distributions in the plasmas of carbon-containing materials – graphite (a), vitreous carbon (b), pyrolitic graphite (c), pencil core (d), silicon carbide (e), and boron carbide (f).

Table 2. Conversion efficiencies in plasmas of carbon-containing materials ($\times 10^{-6}$).

Harmonic number	Wavelength/ nm	Sn	Zn	Mn	Ti	Cu	W	Au	B	Ta	Ag	Cr	Mo	Si	Al
5	213	100	80	80	70	46	46	40	40	26	20	20	4.2	3.83	6
7	152	66	66	20	20	33	40	33	13	10	16	7.1	3.8	1.75	2.59
9	118	66	53	10	12	15	38	26	3	3	10	3.8	2.5	1.75	1.33
11	97	53	40	6.6	6.6	13	33	20	1.3	1.8	6.6	3.8	2.1	0.91	
13	82	26	4	2.1	4.6	2.5	7	1.8	1	0.9	2.6	1.3	0.9	0.91	
15	71	16	4	1.75	3.3	0.9	5	1.3		0.9	1.3	0.9			
17	63	6	1.7	1.3	2.1	0.9		1.3		0.9	1	0.9			
19	56	6	1.7	1.3	2.1	0.83		0.9		0.75	1	0.9			
21	51	4	1	1.3	2.1	0.75		0.9		0.75	1	0.9			

beginning with the minimal (7×10^{12} W cm^{-2}) probe radiation intensity whereby the harmonic signals are safely recorded and ending with the highest intensity (4×10^{13} W cm^{-2}). In particular, in the pyrolitic graphite plasma at probing radiation intensities of 1.2, 2.5, and 3.7×10^{13} W cm^{-2} the 7th-to-5th harmonic signal ratio was equal to 5.5, 4.5, and 8.3, respectively. In this case, in the intensity range under investigation the dependence of the 7th harmonic signal on the probing radiation intensity was close to a quadratic power law. Beginning with 10^{13} W cm^{-2}, the exponent lowered to unity, but it increased in the range from 2.5 to 3×10^{13} W cm^{-2}; subsequently it lowered with increase in probing radiation intensity once again. The dependence of the 5th harmonic signal on the probing radiation intensity was also close to a second-order power law, whose exponent lowered when the probing radiation intensity exceeded 2×10^{13} W cm^{-2}. Therefore, the dependences of the 5th and 7th harmonic intensities on the probing radiation intensity exhibit saturation, which markedly distinguishes them from the traditional power law dependences of the 5th and 7th harmonic signals.

According to the ordinary perturbation theory, which is valid when the field intensity is lower than the intra-atomic field, the intensity of each next-in-order harmonic should be lower in intensity than the previous one [21]. The signal of the 7th harmonic was nevertheless observed to be higher than the 5th harmonic signal in practically all carbon-containing materials (Fig. 7). An exception was provided by the plasma generated on the surface of boron carbide (Fig. 7f). Another special feature of HOHG in the plasmas of carbon-containing materials is the relatively low signal of the 5th harmonic relative to the 9th one. Possible reasons for this behaviour are discussed below. The efficiencies of HOHG in the plasmas produced on the surface of carbon-containing materials are collected in Table 2.

6. Discussion of results

Our investigations have demonstrated high efficiencies of radiation conversion to low-order harmonics, which creates the necessary prerequisites for the development of a high-efficiency coherent radiation source in the 100–200-nm spectral range. Metals like Sn, Zn, Mn, and Ti are better suited for the production of higher efficiencies of picosecond radiation conversion. In several materials the measured 7th harmonic (152 nm) generation efficiencies amounted to $\sim 10^{-4}$. In Sn plasmas the efficiency of conversion to the 11th harmonic (97 nm) was only two times lower and amounted to $\sim 0.5 \times 10^{-4}$. We note that in the remaining materials, too, the efficiencies of conversion to harmonics ranging from the 13th to the 21st ranged from 10^{-5} to 10^{-6}.

The efficiency of radiation conversion in the plasma of carbon-containing materials was approximately one order of magnitude lower than in the plasmas produced on the surface of metals. The exception was provided by the 7th harmonic,

whose generation efficiency was comparable to that in the metal plasmas. The relative increase in the 7th harmonic signal and the lowering of the 5th harmonic signal may be caused by absorption of the latter. However, an earlier analysis demonstrated the absence of absorption in carbon at the 5th harmonic wavelength (λ = 213 nm) [24], which should prevent the relative lowering of its signal. We note that the dependence of harmonic signals on the probing radiation intensity saturated and did not correspond to the power law with exponent of the order of the harmonic number.

A change of the nonlinear response at certain radiation frequencies is possible due to resonance transitions in atoms and ions. Carbon atoms and ions have several transitions with wavelengths close to the wavelength of the 7th harmonic (λ = 152 nm) of Nd:YAG laser radiation. Among them are: $2s^2 2p^2\,{}^1D - 2s^2 2p\ 3d\,{}^1D^0$ (C I, λ = 148.2 nm), $2s^2 2p^2\,{}^3P - 2s\,2p^3\,{}^3D^0$ (CI, λ = 156.0 nm), and $1s^2 2s\,{}^2S - 1s^2 2p\,{}^2P^0$ (C IV, λ = 154.8 nm) [24]. In early works on the HOHG at low-order nonlinearities, an intensive study was made of the use of atomic resonances to improve the efficiency of laser radiation conversion (see, for instance, paper [21] and references therein). In particular, it was shown that the 5th harmonic signal exceeded that of the 3rd harmonic of 266-nm radiation (the 4th harmonic of Nd:YAG laser radiation) in helium due to the increase in fifth-order nonlinearity close to resonance [25]. A theoretical analysis of the feasibility of realising resonance conditions for HOHG in a plateau region in gas media, which was performed during the last decade, revealed that this technique shows promise for improving the efficiency of harmonic generation [26–30]. However, experimental research aimed at realising the resonance enhancement of harmonics in gas media did not bear out this possibility.

A much wider (in comparison with gases) choice of plasmas makes plasma media more promising. Even the first investigations in these media, which were performed with different targets under optimised excitation, showed a rise in the efficiency of generation for individual harmonics near the resonance transitions of these materials [31–33]. In particular, observed in indium plasmas was a significant (200-fold) increase in intensity of the 13th harmonic (λ = 61 nm) of femtosecond Ti:sapphire laser radiation (λ = 790 nm), which was caused by the effect of a strong transition to an autoionisation state [31]. To confirm the influence of resonance transitions, use was made of wavelength tuning of the broadband laser radiation or of a variation of the pulse chirp. However, this technique is not applicable in the case of narrow-band Nd:YAG laser radiation.

Recent attempts undertaken to provide a theoretical explanation for the observed experimental results, namely the increase in intensity of a single harmonic under resonance condition [34–40], showed that the efficiency of HOHG by a single atom or ion is substantially higher near resonance in the framework of the three- and four-stage models as well as of the model involving a superposition of resonance states. The resultant increase in individual harmonic efficiencies was close to experimental data. As shown in Ref. [35], the influence of autoionisation states on phase matching may lead to an efficient enhancement of the 21st harmonic in calcium plasmas and its efficiency of $\sim 10^{-3}$. Therefore, the growth of efficiency under resonance conditions depends heavily on the nonlinear interaction of the waves in the course of their propagation as well as on the variation of response of an individual particle.

Below we estimate the contributions of the resonance enhancement of nonlinear susceptibility and the nonlinear wave interaction in the framework of the perturbation theory (in our case, the maximum amplitude of the laser field was $\sim$30 times lower than the intra-atomic field of carbon atoms). As discussed above, the nonlinear medium consists primarily of neutral atoms and singly charged carbon ions. The presence of free electrons also increases the level of variability of the parameters of the plasma medium. Carbon atoms can reside in singlet and triplet states. According to estimates made proceeding from an analysis of transitions from the initial ground state of carbon atoms, the ratio between the absolute values of the 7th and 5th order nonlinearities $r = |\chi^{(7)}/\chi^{(5)}|$, which are responsible for the harmonics generation, does not exceed 7×10^{-12} CGSE units. In the calculation of nonlinearities based on well-known expressions (see, for instance, Ref. [21]), the values of transition frequencies and oscillator strengths were borrowed from the tables of Ref. [24]; to avoid uncertainty in the sign of the corresponding matrix element of the dipole moment operator, we included only even combinations for transitions between atomic and ionic states. Estimates showed that owing to proximity to resonance conditions (for carbon atoms the mismatch from the seven-photon resonance was equal to $\sim$1690 cm^{-1} both for the triplet state and the singlet one) the seventh-order resonance nonlinearity exceeded the nonresonance nonlinearity by a factor of $\sim$10. We made estimates of harmonics intensity change, using relations borrowed from Refs [14, 21], under the conditions whereby the diffraction probing beam length exceeded the plasma dimension. The effect of phase mismatch was neglected. Assuming the above nonlinearity ratio r and a peak probing radiation intensity $I = 7 \times 10^{12}$ W cm^{-2}, the 7th-to-5th harmonic intensity ratio $\gamma = I_7/I_5$ did not exceed 3×10^{-2}. Therefore, estimates for a single carbon atom suggest that the 5th harmonic intensity should exceed the 7th harmonic intensity in the pump intensity range under investigation.

For the 7th harmonic signal to exceed the 5th one at an intensity $I = 0.7 \times 10^{13}$ W cm^{-2}, the ratio r must be higher by one order of magnitude. This is possible, as follows from a comparison of calculated and experimental high-order nonlinearity values. However, as the probing radiation intensity increases to its maximum value ($I = 4 \times 10^{13}$ W cm^{-2}) the intensity ratio must increase by a factor of $\sim$35, which was not observed in the experiment. The signals both of the 5th and of the 7th harmonics saturated with increasing probing radiation intensity.

Let us consider the processes which may lead to a change and saturation of the efficiency of harmonic generation in the nonlinear wave interaction. The values of the phase mismatch $\Delta k_q = k_q - k_1$ (here, k_q is the qth harmonic wavenumber) for the 5th and 7th harmonics are positive for carbon ions and carbon atoms in the ground singlet state. The phase mismatch due to the electron gas is also positive. Consequently, the total phase mismatch in the plasma should be positive in this case. The phase mismatch for the 7th harmonic due to carbon atoms residing in the initial ground triplet state is negative. An addition of 5% of the electron gas and carbon ions is capable of phase matching the 7th harmonic to the fundamental radiation in this medium. At the same time, the phase mismatch Δk_5 for the 5th harmonic increases. For large mismatches the dependences of harmonic intensities on the length of the medium assumes an oscillatory character, and the signal of the 5th harmonic may be suppressed and may become lower than the 7th harmonic signal. According to our calcula-

tions, for a plasma length of 0.5 mm this situation takes place when the density of carbon atoms residing in the ground triplet state is equal to 1.2×10^{19} cm^{-3}, which is one order of magnitude higher than the estimated plasma density.

The effect of linear phase mismatch Δk_q does not change the power-law dependence of harmonic signals on the probing radiation intensity. Under resonance conditions, its saturation may be caused by the Stark shift of the resonance level or the saturation of the resonance transition. However, when the detuning from resonance is equal to 1690 cm^{-1} these factors can hardly play a significant role. Under nonresonance conditions, the saturation and the subsequent oscillations may arise from Kerr nonlinearities, i.e. from the intensity-dependent change of the refractive index of the medium at the fundamental and harmonic frequencies. Estimates of the Kerr nonlinearities made on the basis of the data of Refs [21, 41] suggest that for carbon atoms residing in the ground singlet state the nonlinear phase mismatches for the 7th and 5th harmonics are of the same sign, while for the triplet state they are opposite in sign and somewhat smaller in absolute value. In the latter case the nonlinear mismatch for the 7th harmonic compensates for the linear mismatch due to the free electrons. In this connection, in the vicinity of the plasma density in use [$(1-2) \times 10^{18}$ cm^{-3}], and when the ratios of the triplet atomic state density to the singlet atomic state density and to the density of singly charged ions (and free electrons) are equal to about 0.3, there exists a relatively broad range of medium parameters whereby the 7th harmonic intensity exceeds the 5th one. In this case, the nonlinear phase shift is responsible for the saturation of both harmonic signals.

It is noteworthy that the nonlinear phase mismatch for the 9th harmonic which arises from carbon atoms residing in singlet and triplet ground states is negative. This compensates for the phase mismatch which arises from the free electrons and makes it possible to enhance the 9th harmonic signal relative to the 5th one.

Our estimates also confirmed the picture of HOHG observed in the plasma which was generated on the surface of boron carbide. In comparison with carbon, a boron atom exhibits much greater nonlinearities, which are responsible both for harmonic generation and for variations of the refractive index. Considering that the atomic binding energy of boron carbide is higher and, consequently, the density of laser plasma is lower, and that the number of atoms and ions of boron is four times greater than that of carbon, the character of nonlinear interaction and the efficiency of HOHG must be quite different.

Recall that one of the first observations of HOHG (up to the 21-order harmonics) in gases, which stimulated interest in this area of nonlinear optics, was also made using Nd:YAG laser radiation with an intensity of 3×10^{13} W cm^{-2} [1]. Our investigations showed that using plasmas produced on the surfaces of different targets as the nonlinear medium can improve the technique of generating coherent radiation in the vacuum ultraviolet, in particular due to a higher energy of picosecond probe radiation in comparison with femtosecond lasers and a wider choice of target materials.

7. Conclusions

In the present work we outlined experimental data on the generation of high-order harmonics of relatively long pulses (in comparison with those employed earlier) of moderate-intensity laser radiation in plasmas produced by simple laser ablation of metal and carbon-containing material surfaces. We demonstrated that the frequency of picosecond Nd:YAG laser radiation can be efficiently converted in metal plasmas to high-order harmonics with a high energy of pulses in the 50–220-nm spectral range. In particular, the efficiency of conversion to the 11th harmonic (λ = 97 nm) in tin plasma was equal to $\sim 0.5 \times 10^{-4}$. For the majority of plasmas, the conversion efficiency for harmonics ranging in order from 13 to 21 was equal to $\sim 10^{-5} - 10^{-6}$. An interesting feature of these investigations consisted in that the observed 7th harmonic (λ = 152 nm) intensity exceeded the 5th one in the plasmas of carbon-containing materials. It was shown that a nonlinear phase mismatch in the carbon plasma is responsible for the saturation of harmonic signals and makes the 7th harmonic stronger than the 5th one over a broad range of laser radiation intensities, plasma densities, and plasma compositions.

Acknowledgements. This work was supported in part by the Third World Academy of Sciences (TWAS) (Grant No. 09-113 RG/PHYS/AS_G).

References

1. Ferray M., L'Huillier A., Li X.F., Lompre L.A., Mainfray G., Manus C. *J. Phys. B: At. Mol. Opt. Phys.*, **21**, L31 (1988).
2. McPherson A., Gibson G., Jara H., Johann U., Luk T.S., McIntyre I., Boyer K., Rhodes C.K. *J. Opt. Soc. Am. B*, **4**, 595 (1987).
3. Norreys P.A., Zepf M., Moustaizis S., Fews A.P., Zhang J., Lee P., Bakarezos M., Danson C.N., Dyson A., Gibbon P., Loukakos P., Neely D., Walsh F.N., Wark J.S., Dangor A.E. *Phys. Rev. Lett.*, **76**, 1832 (1996).
4. Vozzi C., Calegari F., Frassetto F., Negro M., Poletto L., Sansone G., Villoresi P., Nisoli M., De Silvestri S., Stagira S. *Laser Phys.*, **20**, 1019 (2010).
5. Desai T., Daido H., Suzuki M., Sakaya N., Guerreiro A.P., Mima K. *Laser Part. Beams*, **19**, 241 (2001).
6. Kur E., Dunning D.J., McNeil B.W.J., Wurtele J., Zholents A.A. *New J. Phys.*, **13**, 063012 (2011).
7. Paul P.M., Toma E.S., Breger P., Mullot G., Auge F., Balcou P., Muller H.G., Agostini P. *Science*, **292**, 1689 (2001).
8. Faldon M.E., Hutchinson M.H.R., Marangos J.P., Muffett J.E., Smith R.A., Tisch J.W.G., Wahlström C.-G. *J. Opt. Soc. Am. B*, **9**, 2094 (1992).
9. L'Huillier A., Balcou P. *Laser Phys.*, **3**, 654 (1993).
10. Krause J.L., Schafer K.J., Kulander K.C. *Phys. Rev. Lett.*, **68**, 3535 (1992).
11. Akiyama Y., Midorikawa K., Matsunawa Y., Nagata Y., Obara M., Tashiro H., Toyoda K. *Phys. Rev. Lett.*, **69**, 2176 (1992).
12. Theobald W., Wülker C., Schäfer F.P., Chichkov B.N. *Opt. Commun.*, **120**, 177 (1995).
13. Wahlström C.-G., Borgström S., Larsson J., Pettersson S.-G. *Phys. Rev. A*, **51**, 585 (1995).
14. Ganeev R.A., Kulagin I.A., Suzuki M., Baba M., Kuroda H. *Opt. Commun.*, **249**, 569 (2005).
15. Ganeev R.A., Singhal H., Naik P.A., Kulagin I.A., Redkin P.V., Chakera J.A., Tayyab M., Khan R.A., Gupta P.D. *Phys. Rev. A*, **80**, 033845 (2009).
16. Ganeev R.A., Singhal H., Naik P.A., Arora V., Chakravarty U., Chakera J.A., Khan R.A., Kulagin I.A., Redkin P.V., Raghuramaiah M., Gupta P.D. *Phys. Rev. A*, **74**, 063824 (2006).
17. Ganeev R.A., Elouga Bom L.B., Kieffer J.-C., Suzuki M., Kuroda H., Ozaki T. *Phys. Rev. A*, **76**, 023831 (2007).
18. Gaudiosi D.M., Reagan B., Popmintchev T., Grisham M., Berrill M., Cohen O., Walker B.C., Murnane M.M., Kapteyn H.C., Rocca J.J. *Phys. Rev. Lett.*, **96**, 203001 (2006).
19. Heckl O.H., Baer C.R.E., Kränkel C., Marchese S.V., Schapper F., Holler M., Südmeyer T., Robinson J.S.,

Tisch J.W.G., Couny F., Light P., Benabid F., Keller U. *Appl. Phys. B*, **97**, 369 (2009).
20. Haessler S., Elouga Bom L.B., Gobert O., Hergott J.-F., Lepetit F., Perdrix M., Carre B., Ozaki T., Salieres P. *J. Phys. B: At. Mol. Opt. Phys*., **45**, 074012 (2012).
21. Reintjes J.F. *Nonlinear Optical Parametric Processes in Liquids and Gases* (New York: Academic Press, 1984; Moscow: Mir, 1987).
22. Anisimov S.I., Imas Ya.A., Romanov G.S., Khodyko Yu.V. *Deistvie izlucheniya bol'shoi moshchnosti na metally* (Influence of High-Intensity Radiation on Metals) (Moscow: Nauka, 1970).
23. Ganeev R.A. *J. Phys. B: At. Mol. Opt. Phys*., **40**, R213 (2007).
24. http://physics.nist.gov/asd
25. Reintjes J., She C.Y. *Opt. Commun*., **27**, 469 (1978).
26. Taieb R., Veniard V., Wassaf J., Maquet A. *Phys. Rev. A*, **68**, 033403 (2003).
27. Gaarde M.B., Schafer K.J. *Phys. Rev. A*, **64**, 013820 (2001).
28. Toma E.S., Antoine P., de Bohan A., Muller H.G. *J. Phys. B: At. Mol. Opt. Phys*., **32**, 5843 (1999).
29. Zeng Z., Li R., Cheng Y., Yu W., Xu Z. *Phys. Scripta*, **66**, 321 (2002).
30. Bartels R., Backus S., Zeek E., Misoguti L., Vdovin G., Christov I.P., Murnane M.M., Kapteyn H.C. *Nature*, **406**, 164 (2000).
31. Ganeev R.A., Suzuki M., Baba M., Kuroda H., Ozaki T. *Opt. Lett*., **31**, 1699 (2006).
32. Ganeev R.A., Naik P.A., Singhal H., Chakera J.A., Gupta P.D. *Opt. Lett*., **32**, 65 (2007).
33. Ganeev R.A. *Open Spectrosc. J*., **3**, 1 (2009).
34. Milošević D.B. *J. Phys. B: At. Mol. Opt. Phys*., **40**, 3367 (2007).
35. Kulagin I.A., Usmanov T. *Opt. Lett*., **34**, 2616 (2009).
36. Strelkov V. *Phys. Rev. Lett.*, **104**, 123901 (2010).
37. Milošević D.B. *Phys. Rev. A*, **81**, 023802 (2010).
38. Frolov M.V., Manakov N.L., Starace A.F. *Phys. Rev. A*, **82**, 023424 (2010).
39. Redkin P.V., Danailov M., Ganeev R.A. *Phys. Rev. A*, **84**, 013407 (2011).
40. Tudorovskaya M., Lein M. *Phys. Rev. A*, **84**, 013430 (2011).
41. Kulagin I.A., Usmanov T. *Kvantovaya Elektron*., **30**, 520 (2000) [*Quantum Electron.*, **30**, 520 (2000)].